

A Microwave Circuit Model for a Magnetostatic Wave Filter

Steven N. Stitzer
Westinghouse Electric Corp.
Baltimore, MD 21203

Abstract

A new circuit model for a magnetostatic forward volume wave filter element is described. The model accurately predicts bandpass shape and triple transit ripple. Computed results are in good agreement with measured performance in an experimental device.

Introduction

Multiple channel filterbanks have many applications as signal sorters in ECM systems. These devices have a single input and a separate output for each channel. One promising technology for this function uses magnetostatic waves (MSW)¹. In one approach, a number of thin strips of epitaxially-grown YIG films are coupled to a common input manifold. Each strip is subjected to a different bias field, thereby producing a different passband frequency. Each YIG strip has its own separate output transducer.

Optimization of the filterbank requires that the YIG filter elements be modeled using conventional resistors, capacitors, inductors, and transmission lines. A previous model described by Owens, et al², treated the transducers as three-ports. The present model uses a similar approach, but the effect of the MSW reflected from the end of the YIG film is absorbed into the expression for the radiation impedance of the transducer. Also, the present model allows the transducers to be terminated in an arbitrary impedance. This is a requirement for a filter element in which the input transducer is part of a manifold common to a large number of filters tuned to different frequencies. Finally, this model has been used to evaluate the effects of external microwave matching networks on the insertion loss and ripple due to triple transit.

Transducer Calculations

A cross sectional view of the transducer and YIG film is shown in figure 1. The basis of the present model is the calculation of the loading in the microstrip caused by excitation of MSW. The calculation of the radiation resistance^{3,4} takes into account the dimensions of the microstrip, substrate, and YIG film along with the magnetic parameters of the ferrite. A uniform bias field is applied perpendicular to the surface of the YIG film. The internal static magnetic field rises rapidly near the end of the film because of demagnetization effects. RF current flowing in the microstrip causes magnetostatic forward volume waves to be launched in both the +x and -x directions. The wave

launched in the -x direction experiences a total phase shift⁵

$$\phi = \int_0^{-x_c} \vec{k} \cdot d\vec{x} \quad (1)$$

between the transducer and the point $-x_c$ at which cutoff ($k=0$) occurs.

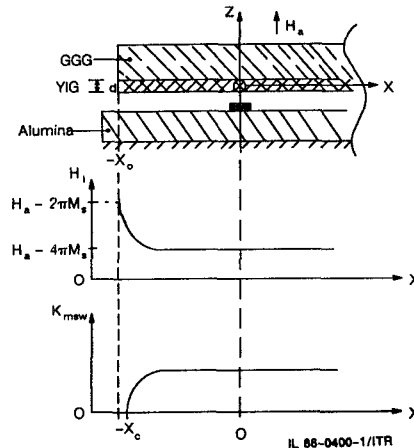


Figure 1. Geometry, internal bias field, and local MSW wave number in a YIG film in the vicinity of a microstrip transducer.

The wave traveling to the right of the transducer is the sum of the direct and reflected waves: $\exp(jkx) - \exp(j(kx + 2\phi))$. This may be rewritten as $2 \sin(\phi) \exp(j(kx - \phi + \pi/2))$. Since, for a given current in the microstrip, the radiation resistance varies as the square of the amplitude of the launched wave, we can define an effective transducer radiation resistance (per unit length):

$$R_T(\omega) = R(\omega) (2 \sin \phi)^2 \quad (2)$$

where $R(\omega)$ is the radiation resistance per unit length of a transducer on an infinitely long YIG film with a uniform internal DC field.

Figure 2 shows calculated values of $R_T(\omega)$ for a 0.5 mm wide microstrip line on a 254 μ m thick alumina substrate, coupled to a 12.5 micron thick YIG film, in a 2814 oersted bias field. The spacing between the YIG film and the microstrip is 160 μ m. The effect of the end reflection is to round off the sharp peak of radiation resistance at the $k=0$ cutoff frequency. In practice, the distance between the transducer and the end of the YIG film is adjusted to smooth the lower edge of the MSW filter passband and minimize sidelobe levels on the upper edge. In the case evaluated here, x_c is approximately 1.5 mm.

The radiation reactance is computed as the Hilbert transform of the radiation resistance:⁶

$$X_T(\omega) = \frac{1}{\pi} \int_{-\infty}^{\infty} \frac{R_T(\omega') - R_T(\omega)}{\omega' - \omega} d\omega' \quad (3)$$

Work performed in part under U. S. Navy contract N00014-85-C-2586.

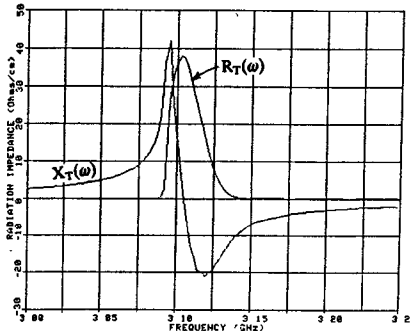


Figure 2. Radiation Impedance $R_T(\omega) + jX_T(\omega)$ of a YIG film

A simplified schematic of a complete single channel of an MSW filter bank is shown in figure 3.

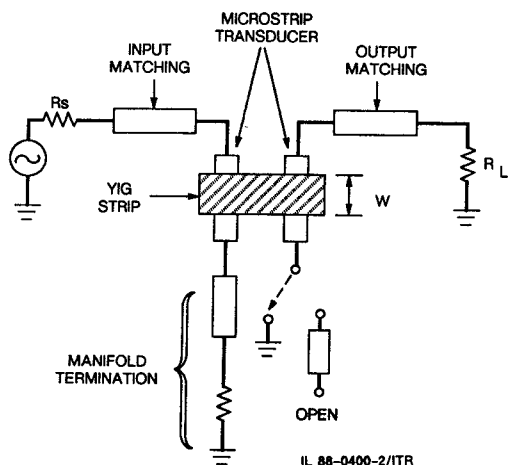


Figure 3. Simplified schematic of an MSW filter. The input transducer is terminated in an arbitrary impedance. The output transducer is either shorted to ground or terminated in an open stub

At 3 GHz, the electrical length of the portion of this line which is under a 1-mm wide YIG strip is about 9 degrees. Therefore, we can approximate the YIG-loaded transducers with lumped element equivalent circuits.

We replace the YIG loading on the input transducers with a transmission line of characteristic impedance $Z_y = R_T w$, coupled through an ideal transformer.

We join the input and output transducers by a transmission line as shown in figure 4. The electrical length of the resulting line is determined by the MSW phase shift: $\theta = k_{msw} l$, where l is the distance between the input and output transducers. The transmission line is assigned a loss equal to the MSW propagation loss, which is taken to be 0.076 $\Delta H T$ (dB), where ΔH is the YIG linewidth in oersteds and T is the MSW group delay in nanoseconds. For $l = 0.5$ cm, $d = 12.5 \mu\text{m}$, the group delay is about 65 nsec. Assuming a typical value for the linewidth of $\Delta H = 0.5$ oersted, the MSW propagation loss is about 2.3 dB.

Below the MSFWW $k=0$ cutoff frequency, we have $R_T=0$, and therefore $Z_y=0$. In this region, the transmission line effectively disappears, and the input and output transducers are completely

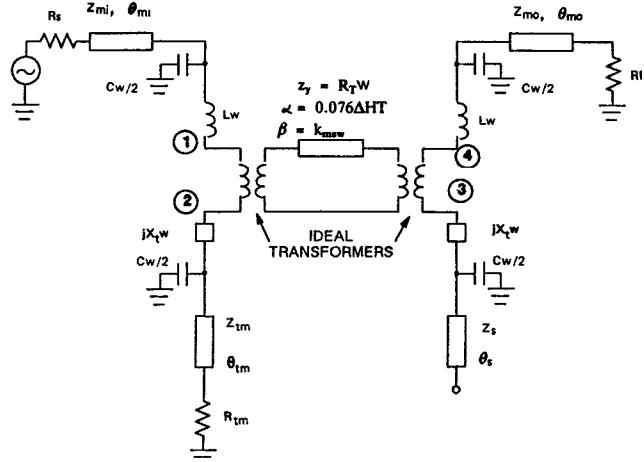


Figure 4. Equivalent circuit of MSW channel

isolated from each other, except for the direct electromagnetic feedthru between the transducers, which is ignored here. However, the non-zero reactance X_T remains in the circuit.

Circuit Analysis

The circuit in figure 4 could be solved by a conventional nodal network analysis, but we can go a step further and reduce the circuit to a more easily handled ladder network. The impedance of the elements between node 2 and ground in figure 4 can be written as

$$Z_2 = jX_T w + 1/(j\omega Cw/2 + 1/Z_{term}) \quad (4)$$

Similarly, the impedance at node 3 is

$$Z_3 = jX_T w + 1/(j\omega Cw/2 + 1/Z_{sturb}) \quad (5)$$

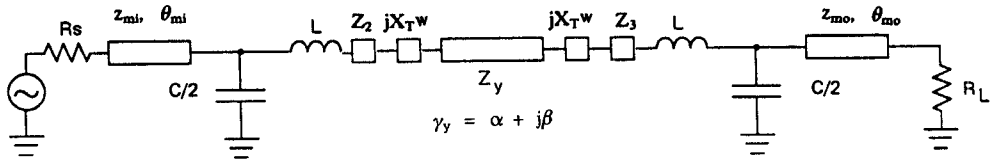
where $Z_{sturb}=0$ for a shorted transducer or $-jZ_s/\tan(\theta_s)$ for an open stub.

Since the current is equal at terminals 1 and 2 of the ideal transformer, we can rearrange the circuit and eliminate the transformers as shown in figure 5.

Figure 6 shows calculated $|S_{21}|$ and $|S_{22}|$ for a typical S-band filter with no matching at the output transducer ($\theta_{mo}=0$). The insertion loss is about 20 dB, with a 3 dB bandwidth of about 20 MHz. The 8 MHz ripple is due to triple transit reflections, with a group delay of about 65 nanoseconds. The lobes on the upper side of the main passband are due to the $J_0(k)/k$ response of the transducer.⁴ Higher order width modes are not considered here because they have been strongly suppressed by depositing a thin layer of aluminum on the YIG film in the experimental devices.⁷

The 50 ohm source is well matched to the input transducer by the manifold matching and termination matching sections. However, the MSW are not well matched to either of the transducers. With an unmatched shorted output transducer, the MSW reflection coefficient is

$$\Gamma_o = (Z_y + jX_T w - R_L)/(Z_y + jX_T w + R_L). \quad (6)$$



$$\begin{bmatrix} A & B \\ C & D \end{bmatrix} = \begin{bmatrix} \cos(\theta_{m1}) & j z_{m1} \sin(\theta_{m1}) \\ j \sin(\theta_{m1})/z_{m1} & \cos(\theta_{m1}) \end{bmatrix} \begin{bmatrix} 1 & 0 \\ j\omega/2 & 1 \end{bmatrix} \begin{bmatrix} 1 & j\omega L + jX_{Tw} + Z_2 \\ 0 & 1 \end{bmatrix} \begin{bmatrix} \cosh(\gamma_L) & z_y \sinh(\gamma_L) \\ \sinh(\gamma_L)/z_y & \cosh(\gamma_L) \end{bmatrix} \begin{bmatrix} 1 & j\omega L + jX_{Tw} + Z_3 \\ 0 & 1 \end{bmatrix} \begin{bmatrix} 1 & 0 \\ j\omega/2 & 1 \end{bmatrix} \begin{bmatrix} \cos(\theta_{m0}) & j z_{m0} \sin(\theta_{m0}) \\ j \sin(\theta_{m0})/z_{m0} & \cos(\theta_{m0}) \end{bmatrix}$$

Figure 5. Ladder equivalent of MSW channel

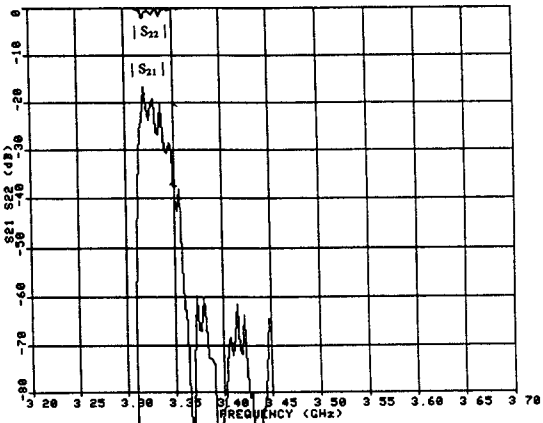


Figure 6. Transmission $|S_{21}|$ and output match $|S_{22}|$ of an MSW filter with a shorted output transducer on an alumina substrate.

Since $Z_y + jX_{Tw}$ is about $6+j9$ ohms at the center of the MSW passband, and $R_L = 50$ ohms, we have $|\Gamma_0| \approx 0.8$, for a return loss of only 1.9 dB. With a similar mismatch at the input transducer, and a two-way MSW propagation loss of 4.6 dB, the triple transit signal will be down only $|\Gamma_0\Gamma_i| \exp(-2\alpha\ell) = 8.4$ dB from the primary signal. This corresponds to a peak-to-peak ripple of about 7 dB.

Two techniques were used to reduce triple transit ripple. The first was to evaporate a thin layer of aluminum on the surface of the YIG film.⁷ Eddy currents flowing in the aluminum layer cause I^2R dissipation of the energy traveling in the MSW, with relatively greater loss taking place in the higher order width modes. However, it also increases the insertion loss of the desired lowest order mode. A constant loss of 6 dB was added to the MSW propagation loss in the computer model to match the calculated loss with the experimentally measured loss. The result of this calculation is shown in figure 7.

In the second technique to reduce triple transit ripple, the output transducer was matched to 50 ohms by a series transmission line, having $z_{mo} = 10.3$ ohms and electrical length $\theta_{mo} = 50$ degrees. The effect of this matching is shown in figure 8. The insertion loss is reduced by about 6 dB and the triple transit ripple is noticeably smaller. This technique is effective over only a very narrow band of frequencies because the impedance of the output transducer

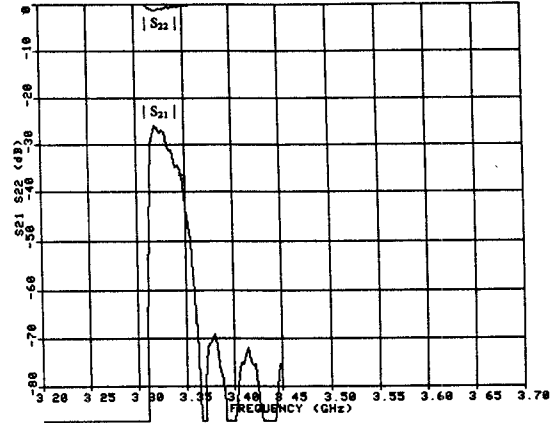


Figure 7. Transmission ripple is reduced when MSW propagation loss is raised by evaporating aluminum onto the YIG surface.

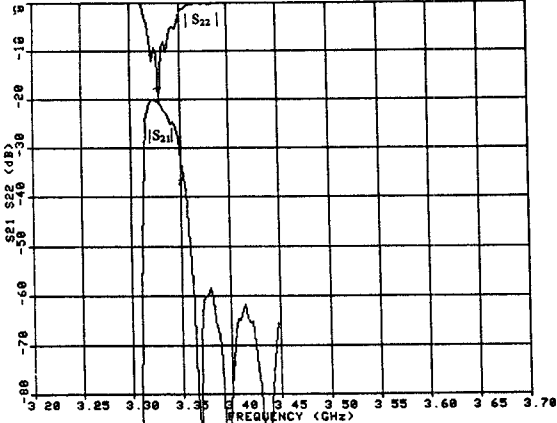


Figure 8. Computed transmission and return loss of an MSW filter with aluminum film and a matched output transducer.

varies much more rapidly with frequency than does that of the low Q matching section.

In a single channel MSW filter, a similar matching circuit could be used at the input transducer to further reduce the insertion loss and ripple. However, this device is intended to become a part of a compact multi-channel filterbank with a large number of channels coupled to a common input manifold. The close physical spacing of the individual channels precludes the possibility of providing separate input matching on each filter section.

It is desirable to place the YIG film over a

current maximum on the microstrip transducer. The input transducer in the filterbank is terminated in a matched load, so the RF current is essentially uniform along its length. The output transducers described above are shorted to ground, and the YIG film is placed as close to the short as possible. We have also evaluated coupling to the midpoint of a half-wavelength open-circuited transducer. Such a transducer can be fabricated in a very small area if a high dielectric constant substrate is used. A 0.5 mm wide microstrip transducer was formed on a 254 μm thick substrate having a dielectric constant of 75, producing an impedance of about 12 ohms. The line from the edge of the YIG to the end of the half-wavelength section length forms an almost perfect matching transformer between the $6+j9$ ohm YIG impedance and the 50 ohm load.

Figure 9 shows computed and measured responses for a single channel built with this type of transducer. The major discrepancies are in the sidelobes, and in the bandwidth. The sidelobes have been suppressed by aluminum strips in the experimental device. The measured upper edge of the passband is in good agreement with the calculations, but the lower edge of the passband has a steeper slope in the calculated results. This may be due to the way we calculate the radiation resistance in the presence of the metallization of the transducer. The effect of the metallization is to raise the $k=0$ cutoff frequency. However, the transducer is very narrow compared to an MSW wavelength at frequencies close

to the bottom of the passband, and so the transducer may not raise the cutoff frequency as much as the present calculation indicates. We plan to investigate this more thoroughly in the future.

Conclusions

A microwave circuit model for magnetostatic wave filters has been developed. The complex radiation impedance of the transducers takes into account the reflection from the open end of the YIG strip. The YIG channel is modeled as a transmission line whose frequency-dependent impedance is equal to the MSW radiation resistance. Triple transit ripple is accurately predicted. The effects of using external matching circuits and thin metal films applied to the YIG for triple transit ripple suppression were discussed.

Acknowledgments

The computer model developed here is based on an earlier program using a simpler model, written by Dr. M.R. Daniel. S.F. Payer provided several enhancements for the program to improve its efficiency and to simplify the preparation of graphic output. I wish to thank Drs. Daniel and J.D. Adam for many helpful discussions, and for preparing the experimental devices.

References

1. J.D. Adam, M.R. Daniel, and S.H. Talisa, "A 13-Channel MSW Filterbank," 1988 MTT-S Symposium.
2. J.M. Owens, R.L. Carter, C.V. Smith, Jr., and G. Hasnian, "A 3-Port Model for Magnetostatic Wave Transducers", Proc. 1980 Ultrasonics Symposium, pp 538-542.
3. A.K. Ganguly and D.C. Webb, "Microstrip Excitation of Magnetostatic Surface Waves: Theory and Experiment", IEEE Trans. MTT-23, December 1975, pp 998-1006.
4. P.R. Emtage, "Interaction of Magnetostatic Waves With a Current", J. Appl. Phys (49)8, August, 1978, pp 4475-4484.
5. J.D. Adam, "An MSW Tunable Bandpass Filter", Proc. 1985 Ultrasonics Symposium, p 157.
6. A.K. Ganguly, D.C. Webb, and C. Banks, "Complex Radiation Impedance of Microstrip-Excited Magnetostatic-Surface Waves", IEEE Trans. MTT-26, June, 1978, pp 444-447.
7. J.D. Adam, Proc. 36th Annual Frequency Control Symposium, 1982, p. 419.

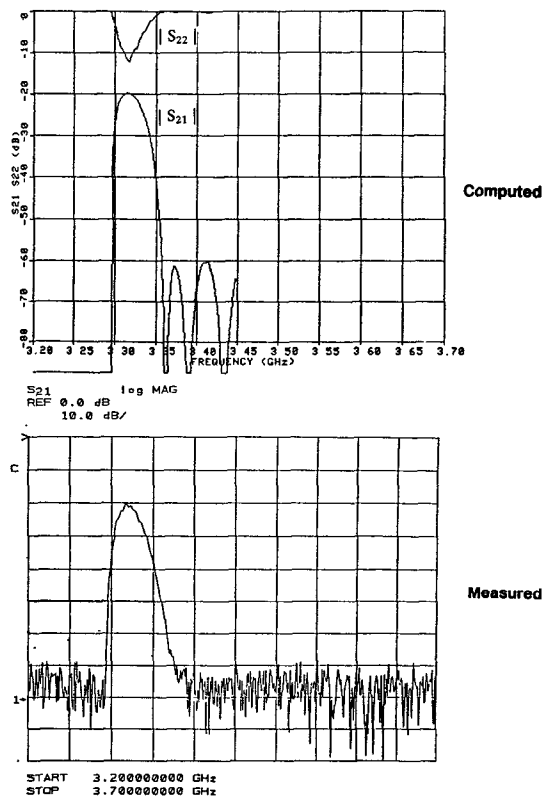


Figure 9. Experimental single channel MSW filter